

Comparison of immune responses to attenuated rabies virus and street virus in mouse brain

Fa-ming Miao¹ · Shou-feng Zhang¹ · Shu-chao Wang¹ · Ye Liu¹ · Fei Zhang¹ · Rong-liang Hu¹

Received: 31 July 2016 / Accepted: 19 September 2016 / Published online: 8 October 2016
© Springer-Verlag Wien 2016

Abstract Rabies is a lethal neurological disease caused by the neurotropic rabies virus (RABV). To investigate the innate immune response in the brain during rabies infection, key gene transcripts indicative of innate immunity in a mouse model system were measured using real-time RT-PCR. Mice were infected via the intracerebral or intramuscular route with either attenuated rabies virus (SRV9) or pathogenic rabies virus (BD06). Infection with SRV9 resulted in the early detection of viral replication and the rapid induction of innate immune response gene expression in the brain. BD06 infection elicited innate immune response gene expression during only the late stage of infection. We measured Na-fluorescein uptake to assess blood-brain barrier (BBB) permeability, which was enhanced during the early stage of SRV9 infection and significantly enhanced during the late stage of BD06 infection. Furthermore, early SRV9 replication increased the maturation and differentiation of dendritic cells (DCs) and B cells in the inguinal lymph nodes and initiated the generation of virus-neutralizing antibodies (VNAs), which cooperate with the innate immune response to eliminate virus from the CNS. However, BD06 infection did not stimulate VNA production; thus, the virus was able to evade the host immune response and cause encephalitis. The rabies virus phosphoprotein has been reported to counteract IFN activation. In an *in vitro* study of the relationship between IFN antagonism and RABV

pathogenicity, we demonstrated that SRV9 more strongly antagonized IFN activity than did BD06. Therefore, there is no positive relationship between the IFN antagonist activity of the virus and its pathogenicity.

Introduction

Rabies is an acute, progressive encephalitis caused by infection with rabies virus (RABV) that presents a public health problem worldwide, causing more than 70,000 human deaths annually [1]. One of the characteristics of RABV is the capacity to enter the central nervous system (CNS). CNS infection with wild-type (wt) RABV is often fatal in humans [2].

Rabies is prevented by prompt post-exposure prophylaxis through the combined administration of the rabies vaccine and a hyperimmune serum containing virus-neutralizing antibodies (VNAs) or immunoglobulin. However, once patients have developed clinical rabies, which is manifested by a CNS infection, the virus cannot be cleared by innate immunity or antibody administration [3]. Currently, the only available treatment for clinical rabies is the “Milwaukee Protocol”; however, due to recent failures, the use of this protocol has been abandoned as an effective treatment for rabies [4, 5]. Despite improvements in our understanding of rabies pathogenesis, clinical rabies remains a fatal disease, and further research is needed to understand the basic mechanism of rabies pathogenesis and to develop an effective treatment.

The innate immune system provides protection against invading neurotropic viruses. It acts as the first line of defense against invading viruses and plays a fundamental role in their pathogenesis [6]. Although the mechanisms by which different RABV strains induce differential immune

✉ Rong-liang Hu
ronglianghu@hotmail.com

¹ Laboratory of Epidemiology, Institute of Military Veterinary, Academy of Military Medical Sciences, Key Laboratory of Jilin Province for Zoonosis Prevention and Control, 666 Liuying West Road, Changchun 130122, Jilin, China

responses are unknown, recent studies indicate that laboratory-attenuated RABV activates the innate immune response of the host, whereas wt RABV evades this response [7]. Therefore, it is clear that virus-specific antibodies are essential for eliminating free virus [8]. However, the interaction between innate immunity and adaptive immunity during a rabies infection is unclear, as is the relationship between the immune response and viral load changes during infection with RABV strains of differing virulence.

In this study, the induction of an immune response was investigated in mice after either intracerebral (IC) or intramuscular (IM) infection with an attenuated rabies virus strain (SRV9) or the pathogenic wt rabies virus strain (BD06). In the early stage of infection after IC administration of SRV9, mice had significantly increased transcript levels of cytokines involved in the innate immune response in the brain compared with mice injected with wt BD06. BD06 inoculation delayed the host immune response until 6 days postinfection (dpi), which was after the appearance of clinical signs. As the infection progressed, wt BD06 evoked greater increases in cytokine transcript levels than SRV9, which coincided with the destruction of the blood-brain barrier (BBB) and a viral load consistent with terminal infection. Following IM infection with SRV9, viral invasion into the CNS initiated innate and adaptive immune responses that eliminated the virus; immune response induction and viral elimination were not observed after IM injection of wt virus. IC or IM injection of SRV9 increased serum VNA levels, whereas no induction of VNAs was observed after injection of wt RABV. Type 1 interferons (IFNs) are important contributors to the defense against viral infection due to their direct antiviral activity [9]. Recent research has shown that viral P proteins suppress IFN responses by antagonizing IFN signaling [10, 11]. To determine whether a positive relationship exists between virus lethality and antagonism of IFN activity by viral P proteins, we evaluated IFN- β antagonism by proteins thought to contribute to RABV immune evasion *in vitro*. Our results showed that the antagonist activity of the wt BD06 virus was stronger than that of the attenuated SRV9 virus.

Characterizing the patterns of different innate immune responses to pathogenic or attenuated RABV infection and the relationship between virus infection and adaptive immunity may improve our understanding of rabies pathogenesis and provide insight into superior therapeutics for rabies.

Materials and methods

Ethics statement

Female BALB/c mice (6 to 8 weeks old) were purchased from Changchun Institute of Biological Products, China.

All animal experiments (including virus maintenance in dogs and suckling mice) described in this study were performed in accordance with established procedures, as defined by the Guidelines on the Humane Treatment of Laboratory Animals stipulated by the Ministry of Science and Technology of the People's Republic of China (MOST) [12], and were approved by the Animal Welfare Committee of the Military Veterinary Research Institute, Changchun, China. All animals were housed in a climate-controlled laboratory with a 12 h/12 h light/dark cycle. No human-patient-derived clinical materials or non-human primates were used in the completion of these studies.

Virus

RABV BD06 (GenBank accession no. EU549783.1) was isolated in our laboratory in 2006 from a rabid dog in China. This virus is maintained in dogs and it was shown in our previous experiments to cause 80 % mortality in unvaccinated dogs after IM injection. In addition, this virus strain is responsible for the majority of rabies cases in humans and dogs in China [13]. SRV9 (GenBank accession no. 499686.2) is a live-attenuated rabies vaccine strain derived from SAD B19 and is nonlethal in adult mice, even after IC administration [14]. Briefly, three-day-old suckling mice received a 30- μ l IC injection of either BD06 or SRV9. Mice were euthanized when they became moribund, and the brains were removed. A 10 % (w/v) suspension was prepared by homogenizing the brains in Dulbecco's modified Eagle's medium (DMEM; Gibco, CA, USA). The homogenates were centrifuged at 12,000 $\times g$ to remove debris, and the supernatant was collected and stored at -80 °C.

Virus infection

All mice were between 4 and 6 weeks of age at the time of infection. For IC inoculation, mice were anesthetized with 100 μ g of ketamine and 1 mg of xylazine per gram of body weight prior to injection with 10⁴ fluorescent focus units (FFU) of SRV9 or BD06. IM inoculation was performed by injecting 10⁷ FFU of SRV9 or BD06 diluted in 100 μ l of DMEM with 10 % fetal bovine serum.

Tissue extraction and total RNA isolation

In the IC experiments, tissue samples were collected at 1, 2, 3, 4, 5, 6, and 7 days postinfection (dpi). In the IM experiments, tissue samples were collected during three time periods: an early phase, which was characterized by an approximately 0.5-g decrease in body weight but no clinical signs of RABV infection; an intermediate phase,

which was characterized by continued weight loss and slight trembling but otherwise normal activity; and a late phase, which was characterized by the appearance of severe clinical signs of rabies, such as paralysis or anger. At each time point, mice were anesthetized with 100 µg of ketamine and 1 mg of xylazine per gram of body weight and killed. The brains were harvested, frozen in liquid nitrogen and stored at -80 °C. Total RNA was extracted from cells in a single-step procedure using TRIzol Reagent (Invitrogen, Life Technologies, USA) according to the manufacturer's protocol. An additional step was performed to remove residual DNA: the aqueous phase was treated with 3 units of RNase-free DNase I for 20 min at 37 °C. RNA purity was determined using a NanoDrop ND-2000c spectrophotometer (NanoDrop Tech, Rockland, DE) to ensure that the A_{260}/A_{280} ratio was within the 1.8–2.0 range. RNA concentration was also determined using a NanoDrop ND-2000c spectrophotometer, and RNA integrity was verified using denaturing agarose gel and polyacrylamide gel electrophoresis.

Quantification of viral loads by RT-PCR and TaqMan RT-PCR

Nested reverse transcription polymerase chain reaction (RT-PCR) was used for semi-quantification of the virus load as described previously [15].

To determine the viral load in the infected brains or locally injected hind muscles, TaqMan qRT-PCR was performed on RNA samples using primers specific for the N gene of rabies virus genotype I (forward, 5'-AGTC AATAATCAGGTGGTCTC-3'; reverse, 5'-ATCTTGCT CCYTTTCGTG-3) and the probe FAM-CCAGTCTTC AGGGCATGTCCCC-TAMRA. TaqMan PCR was performed using a GoTaq[®] Probe 1-Step RT-qPCR System (Promega) in a multiplex Mx3000P qPCR System (Stratagene) according to the manufacturer's instructions. TaqMan analyses of experimental samples contained at least three replicates and included no-template or no-primer controls. The PCR conditions were 45 °C for 15 min for reverse transcription, followed by 95 °C for 2 min, 40 cycles of 95 °C for 15 s and 60 °C for 60 s. A standard curve was generated from serially diluted RABV N RNA of known copy number, and the sample copy numbers were normalized to 1 ng of total RNA. An absolute standard curve method was used to calculate the copy number of RABV N mRNA in the samples [16]. To exclude genomic DNA contamination, control cDNA reactions in which reverse transcriptase was omitted were prepared in parallel as described elsewhere [17], and these reactions were uniformly negative (Table 1).

Table 1 Primer sequences for mouse cytokine genes used in this study

Name	Primer sequence (5'-3')
GAPDH-F	GGAGAAGCTGCCAATGGATA
GAPDH-R	TTACGCTTGCACTTCTGGTG
IFN-β-F	GAACAACAGGTGGATCCTCCA
IFN-β-R	TCCGAGCAGAGATCTTCAGG A
IFIT-1-F	AGGCTGGAGTGTGCTGAGAT
IFIT-1-R	TCTGGATTTAACCGGACAGC
IFIT-2-F	CACCTTCGGTATGGCAACTT
IFIT-2-R	GCAAGGCCTCAGAATCAGAC
OASL1-F	TCCTGGAGGACTGGTTTGAC
OASL1-R	ACTGAAGACGTGGACCATCC
MCP-1-F	AGCCAACTCTCACTGAAGCC
MCP-1-R	TGTGACTCGGACTGTGATGC
IP-10-F	ATGACGGGCCAGTGAGAATG
IP-10-R	CCTCCTTGCTCCTCCCTAGCT
IRF7-F	AGGTTCTGCAGTACAGCCAC
IRF7-R	GCAAGGGTCACCACACTACA
ISG15-F	CGATTCCTGGTGTCCGTGA
ISG15-R	TGATCAAGCATTGCGCCTG
Mx-1-F	CGGCAGAAGCTTGCCAAATT
Mx-1-R	AGACCAGTCCTCTAGGCAGG

Real-time SYBR Green PCR

To confirm expression changes following RABV infection, real-time PCR was performed on the RNA samples using gene-specific primers in a Stratagene Mx3000P qPCR System. RNA was extracted from the supernatants of homogenized brain tissue using an RNeasy Mini Kit (QIAGEN) according to the manufacturer's instructions, and cDNA synthesis was performed using PrimeScript[™] RT Master Mix (Perfect Real Time, Takara) at 37 °C for 25 min. The PCR conditions were as follows: 95 °C for 30 s; 40 cycles of 95 °C for 5 s, 55 °C for 30 s and 72 °C for 30 s; and 95 °C for 15 s, 55 °C for 15 s and 95 °C for 15 s for a melting curve analysis. The expression level of the gene of interest was normalized to the expression of glyceraldehyde-3-phosphate dehydrogenase (GAPDH). All data were analyzed using EcoStudy Software (Agilent Technologies, CA, USA), and mRNA expression levels were calculated using the $2^{-\Delta\Delta C_t}$ method.

Flow cytometry assay and plasmid transfection

Inguinal lymph node samples were collected at the indicated times. Cell suspensions were stained with anti-CD19, anti-CD40, anti-CD11c, and anti-CD80 antibodies. All labeled cells were analyzed using a flow cytometer. Flow

cytometry antibodies and reagents were purchased from BD Pharmingen (BD Biosciences, Franklin, VA, USA).

For transfection, 293Ad cells were seeded into 6-well plates at a density of 10^6 cells/well to yield 70 to 90 % confluency the next day, cultured in Dulbecco's modified Eagle's medium (DMEM, Gibco) supplemented with 10 % fetal bovine serum (FBS, Gibco) and streptomycin-penicillin at 37 °C with 5 % CO₂. Cells were transfected with 1.5 µg of pIRES-neo alone or cotransfected with 0.5 µg of pcDNA-flag-RIG-I-CARDs and 1µg of pIRES-neo, pIRES-SRV9-P or pIRES-BD06-P using FuGENE[®] HD (Promega) according to the supplier's instructions. pEGFP-C1 (Clontech) was used as a transfection efficiency control. Each transfection was performed in duplicate for RNA purification and protein sample preparation.

Assessment of BBB integrity

BBB integrity was assessed by quantifying the BBB leakage of a low-molecular-weight fluorescent marker (Na-fluorescein; molecular weight, 376 Da) from the circulation into the CNS as described previously [18]. Briefly, 100 µl of a 10 % solution of Na-fluorescein was injected intraperitoneally. After 10 min, the mice were anesthetized, cardiac blood was collected, and transcardial perfusion with PBS was performed. The tissue and serum samples were homogenized and centrifuged, and the supernatants were clarified with 15 % trichloroacetic acid. The fluorescence level was measured using a CytoFluorII fluorimeter. The amount of Na-fluorescein in CNS tissue was normalized to the serum levels using the following equation: (µg of Na-fluorescein in CNS tissue/mg of tissue)/(µg of Na-fluorescein in serum/µl of serum).

Statistical analysis

Statistical significance was determined by one-way ANOVA, and a *P*-value less than 0.05 was considered statistically significant. The data are presented as the means ± standard deviations (SDs). Similar results were obtained in at least three independent experiments. Statistically significant differences between groups were analyzing using GraphPad Prism 5.0 software (La Jolla, CA).

Results

Different outcomes in mice infected with SRV9 or BD06 RVs

BALB/c mice were injected (IC or IM) with either SRV9 or BD06 and then monitored for survival. The IC dose of SRV9 or BD06 was 10^4 FFU. The body weights of the

SRV9-infected mice increased slowly prior to 4 dpi, decreased by approximately 5 % at 5 dpi, increased again at 7 dpi, and continued to increase until completion of the study (Fig. 1A). In contrast, the body weights of the BD06-infected mice steadily decreased throughout the experiment (Fig. 1C). In particular, at 5 dpi, the body weights decreased in conjunction with the appearance of tremors, shaking, and anger in the animals, which was later followed by paralysis of one or both hind limbs (see “Materials and methods”). The BD06-infected mice began to die at 6 dpi (with an approximately 18 % body weight decrease), and all of the mice died by 7 dpi (Fig. 1B). The mock-infected and SRV9-infected mice survived throughout the entire experiment (14 dpi, data not shown). The IM dose of SRV9 or BD06 was 10^7 FFU. The body weight changes in SRV9-infected mice were similar after IM or IC injection. For BD06-infected mice, the IM-injected mice lost weight for a longer time period than the IC-injected mice. Of the IM BD06-infected animals, 10 % died by 7 dpi, and all mice succumbed to RABV by 14 dpi (Fig. 1D). Based on these results, we confirmed that BD06 is pathogenic and causes death in all infected mice, whereas SRV9 is a nonlethal RABV strain.

Different innate immunity response profiles in SRV9- and BD06-infected mice

To investigate innate immune responses after infection, the transcript levels of chemokines (MCP-1 and IP-10) and IFN-related genes (IRF7, IFNβ, IFIT1, IFIT2, ISG15, Mx-1, and OASL1) were quantified using qRT-PCR. The mRNA expression of the reference gene GAPDH was also quantified. Each gene was analyzed in replicates of four. In the IC SRV9-infected mice, the expression of eight of the nine selected genes demonstrated a change at 1 dpi, with increasing expression until 5 dpi and then decreased expression at the ED (end point). MCP-1 expression in the SRV9-infected mice was 41-fold higher at 1 dpi and remained at this level until the ED. In the BD06-infected mice, no changes in gene expression were observed until 5 dpi (which coincided with the appearance of trembling). By the ED, all of the selected genes showed large increases in expression (Fig. 2A). Different patterns of gene expression were observed in the IM-injected mice. In the early stage, the SRV9 virus had reached the spinal cord, and a small amount of the virus entered the cerebrum before it was eliminated. In BD06-infected mice, slight changes in the expression of all the target genes (up to a 1- or 2-fold change) were observed in the early stage compared with mock-infected mice. In the intermediate stage, the BD06-infected mice displayed the typical clinical signs of rabies, including trembling and anger, which corresponded to large increases in the transcription of genes involved in innate

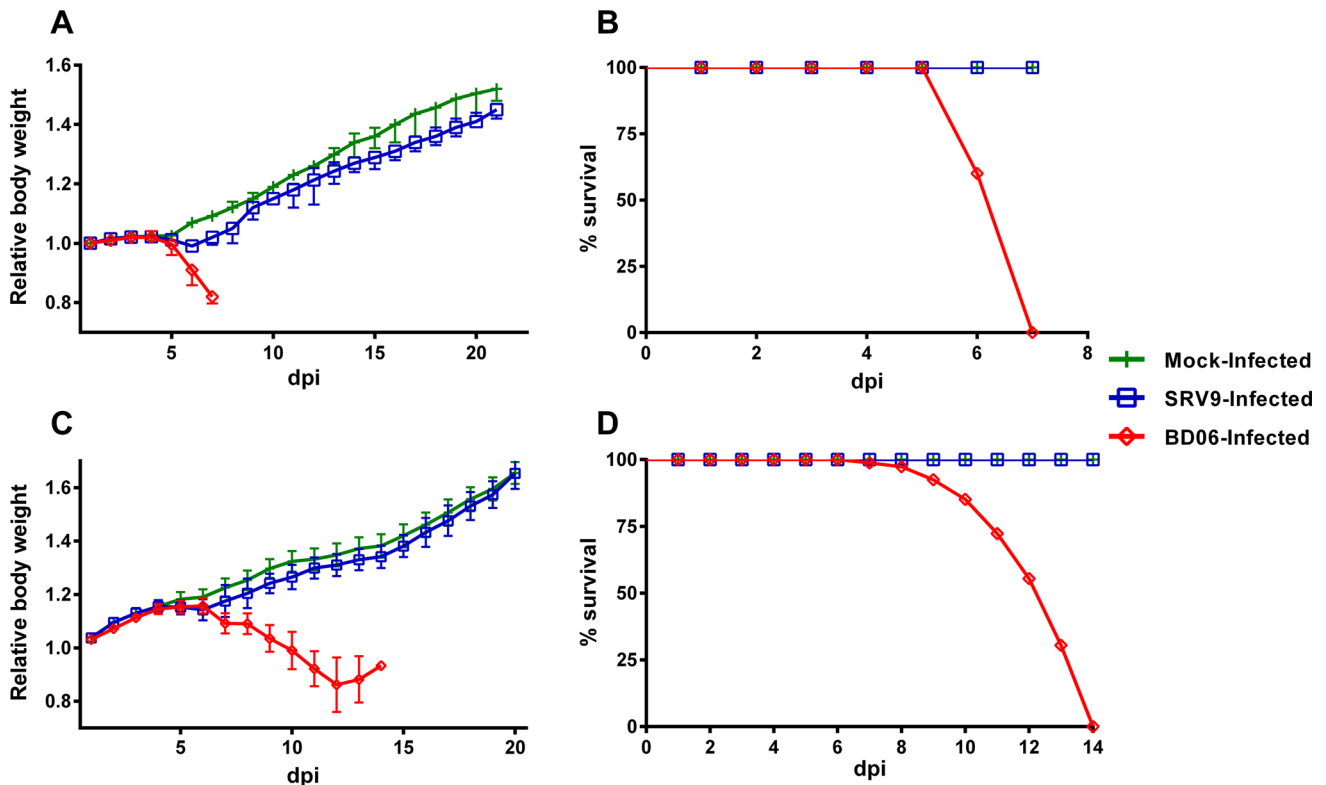


Fig. 1 Comparison of the pathogenicity of the SRV9 and BD06 RABV strains. **(A)** Changes in body weight at the indicated days postinfection (dpi) in mock-, SRV9- and BD06-infected mice after IC injection ($n = 10$). Data are shown as the mean \pm standard deviation (SD). **(B)** Survival rates at the indicated dpi in mock-, SRV9- and

BD06-infected mice after IC injection ($n = 10$). **(C)** Changes in body weight at the indicated dpi in mock-, SRV9- and BD06-infected mice after IM injection ($n = 10$). Data are shown as the mean \pm SD. **(D)** Survival rates at the indicated dpi in mock-, SRV9- and BD06-infected mice after IM injection ($n = 10$)

immunity. By the late stage (corresponding to the ED in the IC-injected mice), further increases in expression were observed for most target genes. These results indicate that in the attenuated SRV9-infected mice, the expression of genes involved in innate immunity initially increased and then decreased to levels similar to those in the mock-infected mice (data not shown), whereas in the wt BD06-infected mice, gene expression slowly increased until the mice displayed clinical signs (Fig. 2B).

A single dose of attenuated SRV9 virus, but not of wt BD06, increased serum VNA levels in infected mice

To investigate the adaptive response of mice after infection, serum samples were collected at various time points and then subjected to a fluorescent antibody virus neutralization test (FAVN) for VNA analysis. The data are expressed as the mean value for the group. As shown in Fig. 3A, the IC SRV9-infected mice had a serum VNA titer of 0.142 IU/ml by 3 dpi; this titer increased to 0.484 IU/ml by 5 dpi, which is close to the titer considered adequate for vaccination or protection by WHO (0.5 IU/ml). However, the BD06-infected mice did not develop a serum VNA titer

until the ED (near death). As shown in Fig. 3B, increased serum VNA levels were observed in the IM SRV9-infected mice at all stages of infection, whereas in the wt BD06-infected mice, little to no serum VNA was observed, even in the terminal stage of infection.

To determine if the increased VNA levels in the SRV9-injected mice correlated with B-cell recruitment, CD19⁺/CD40⁺ B cells from the inguinal lymph nodes were analyzed by flow cytometry. As shown in Fig. 3C, the number of CD19⁺/CD40⁺ B cells increased as a function of time after immunization. The number of CD19⁺/CD40⁺ B cells was significantly increased in the lymph nodes of the SRV9-infected mice compared with the BD06- and mock-infected mice at the intermediate stage of infection. These data indicate that SRV9 infection, but not wt BD06 infection, results in the recruitment of B cells to the lymph nodes.

To determine if B cell recruitment is due to dendritic cell (DC) recruitment, we analyzed CD11c⁺ and CD80⁺ (DC markers) cells in the inguinal lymph nodes. As shown in Fig. 3D, the number of CD11c⁺/CD80⁺ cells in the lymph nodes of the SRV9-infected mice was significantly increased compared with the BD06-infected mice in the intermediate stage of infection. These data show that IM

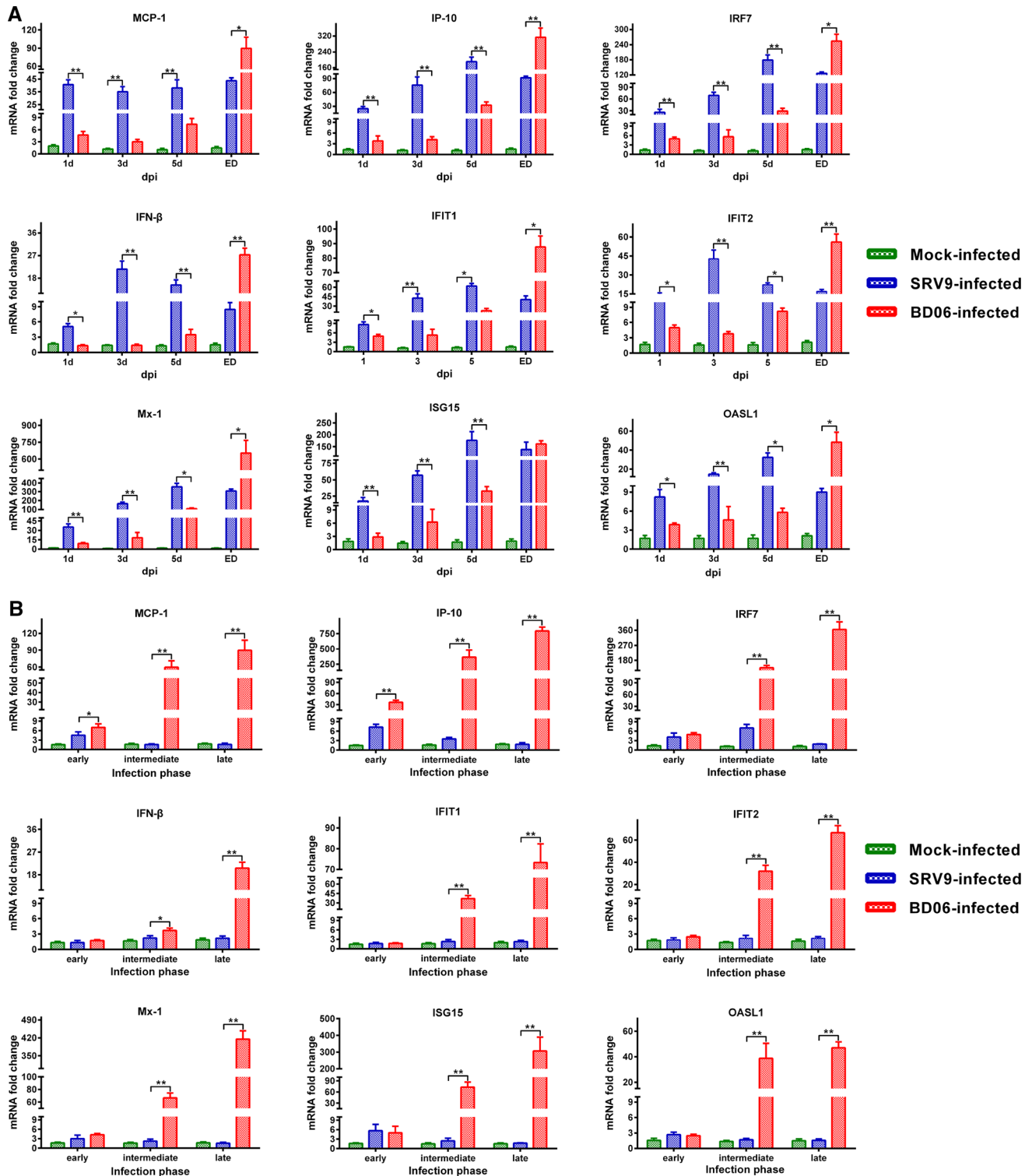


Fig. 2 Comparison of the expression profiles of genes involved in innate immunity in SRV9- and BD06-infected mice. Mouse brains were processed as described in “Materials and methods” and subjected to qRT-PCR for mRNA analysis. Expression levels of

genes involved in innate immunity in SRV9- or BD06-infected mice after IC (A) or IM (B) injection. Statistical significance was determined by one-way ANOVA (*, $P < 0.05$; **, $P < 0.01$)

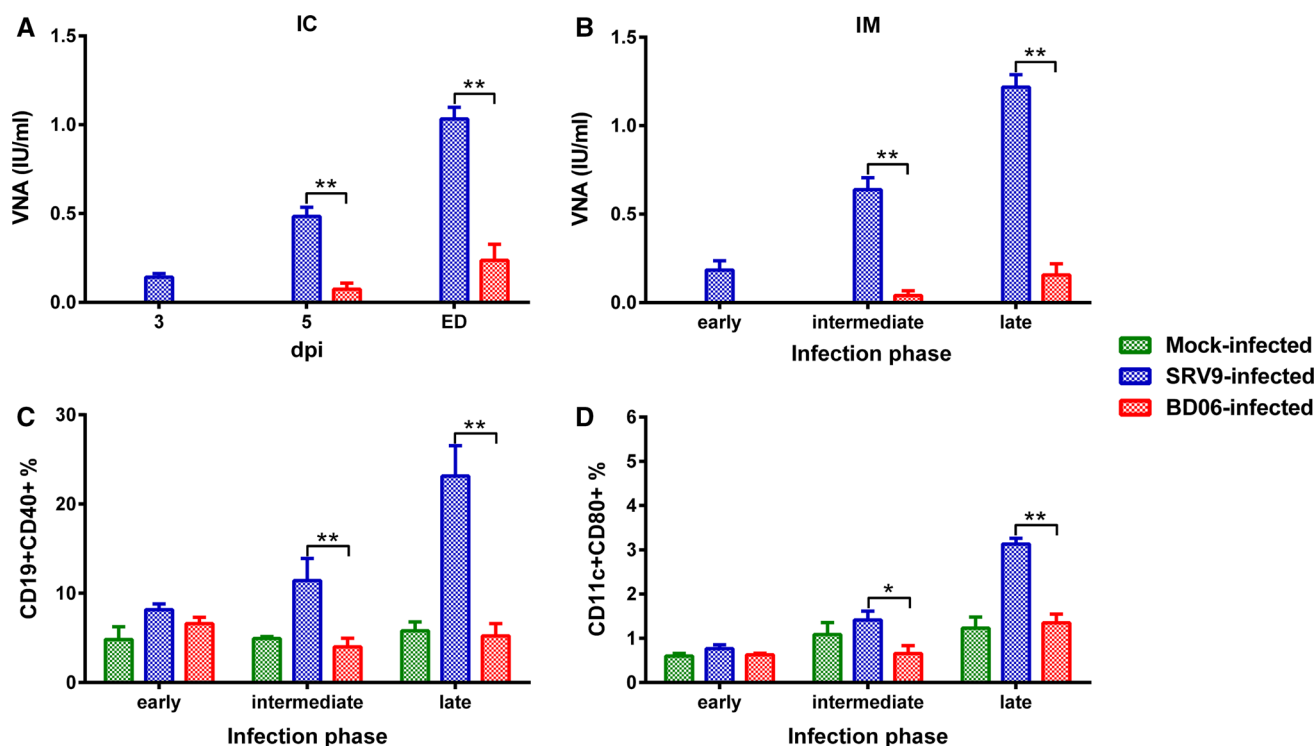


Fig. 3 Comparison of cell-mediated immune responses and VNA levels in mock-, SRV9- and BD06-infected mice after IC or IM injection. (A-B) Serum VNA levels in IC- and IM-injected mice. (C-

D) Flow cytometry analysis of activated B cells and DCs in the lymph nodes of IM-injected mice

injection of SRV9 results in the recruitment of DCs to lymph nodes and peripheral blood.

Viral load in SRV9- or BD06-infected mice via IC or IM injection

To determine if the enhanced innate and adaptive immune responses in the SRV9-infected mice was due to virus replication, we use qRT-PCR and nested RT-PCR to assess RABV nucleotide protein mRNA levels in the cerebellum as a measurement of virus replication. In IC-injected mice, SRV9 adapted in local tissues for one day before it started to replicate. Viral replication stabilized at 4 dpi and then quickly declined. Conversely, BD06 adapted for one day and then slowly replicated (with little to no change) until 4 dpi. After 4 dpi, virus replication quickly increased to 10^6 copies/mg of brain tissue before stabilizing (Fig. 4A-B). In the IM-injected mice, similar viral loads were observed in the injected left hind legs of both the SRV9- and BD06-infected mice; however, the SRV9 virus was eliminated more quickly (Fig. 4C). The BD06 virus was transmitted from the peripheral axons to the CNS as early as 6 dpi; in the BD06-infected brains, viral load initially increased and later decreased. The detailed changes are shown in Fig. 4D.

Comparative analysis of antagonism of IFN- β activity by the lethal and nonlethal RABV strains

To investigate antagonism of IFN- β activity by the lethal and nonlethal RABV strains, plasmids expressing RIG-I-CARDs were used to activate the IFN pathway, and plasmids expressing the P genes of either SRV9 or BD06 were used to transfect IFN-competent 293Ad cells. Expression was verified by Western blotting (Fig. 5A). The mRNA expression levels of IFN- β , PKR and 2-5 OAS in the transfected 293Ad cells were quantified by qRT-PCR. RIG-I increased the expression of IFN- β , PKR and 2-5 OAS compared with the pIRES-Neo (EV) control. Furthermore, the induction of all three proteins was blocked by RABV phosphoproteins, consistent with previous studies [19]. Intriguingly, SRV9 P more robustly suppressed mRNA expression than BD06 P (Fig. 5B). The greater ability of SRV9 P to suppress RIG-I-dependent activation of IFN- β signaling suggests that SRV9 may have an attenuated capacity for continuous IFN induction. These results indicate that although BD06 is more pathogenic than SRV9, BD06 induces a greater IFN response that is not as strongly antagonized by its P protein.

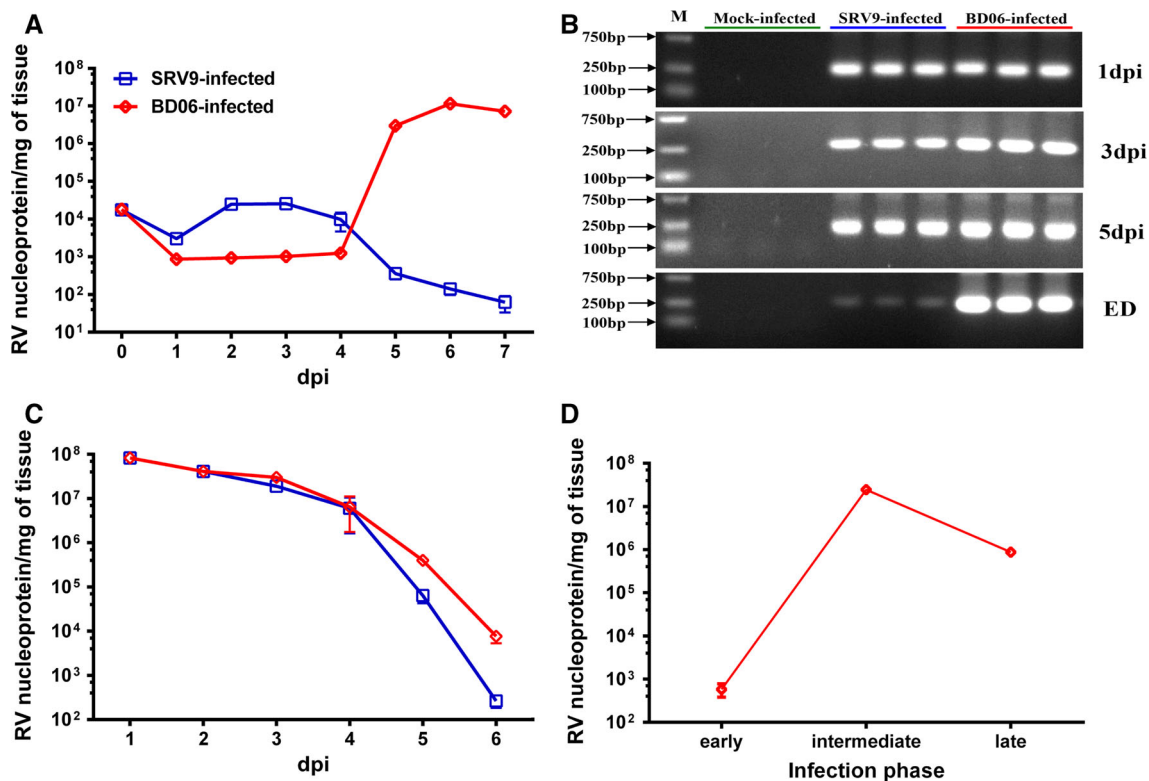


Fig. 4 Viral load comparison in SRV9- or BD06-infected mice after IC or IM injection. (A-B) The number of copies of RABV nucleoprotein per mg of brain tissue, determined in IC-injected mice

using TaqMan qRT-PCR and RT-PCR. (C-D) Quantification of the viral load in infected muscle tissue and brain of IM-injected mice by TaqMan qRT-PCR

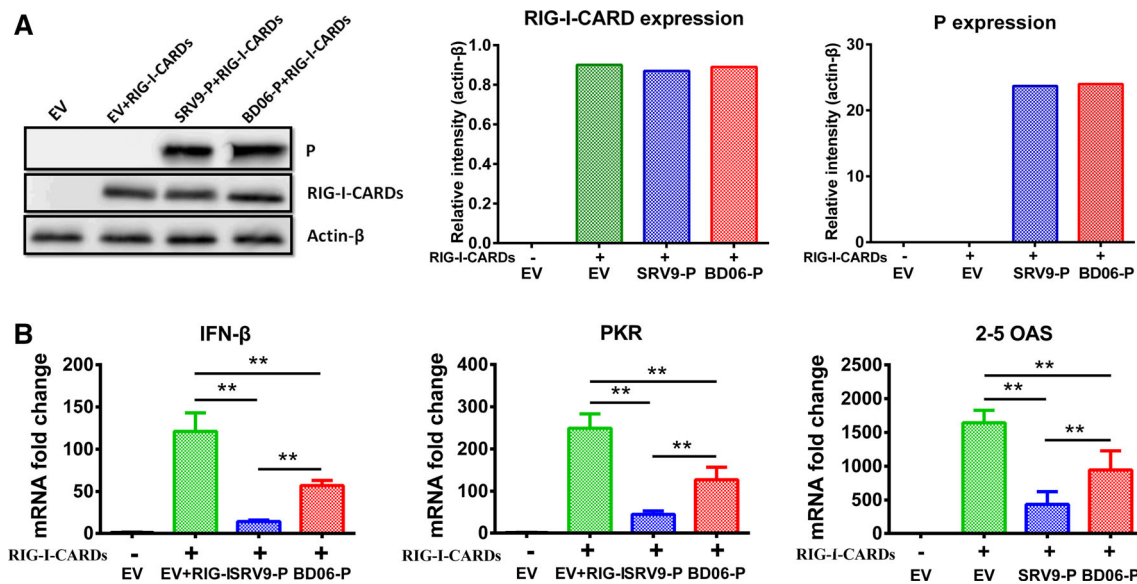


Fig. 5 Comparison of the antagonism of IFN activity by the structural proteins of SRV9 and BD06. 293Ad cells were transfected with 1.5 μ g of pIRES-neo (empty vector, EV) alone or in combination with 0.5 μ g of pcDNA-flag-RIG-I-CARDs (RIG-I-CARDs) and 1 μ g

of either EV, pIRES-SRV9-P (SRV9-P) or pIRES-BD06-P (BD06-P). Expression of RIG-I-CARDs, SRV9-P, and BD06-P (A) and IFN- β , PKR and 2-5 OAS (B) mRNA were quantified

A single IC dose of attenuated SRV9 enhanced the BBB, whereas wt BD06 weakened the BBB in the late stage

To evaluate alterations in BBB permeability following IC injection of either SRV9 or BD06, we analyzed Na-fluorescein extravasation from the circulation into the CNS at 1, 3, and 5 dpi and at the ED and measured Na-fluorescein content using a standard curve. Compared with BD06-infected mice, Na-fluorescein levels were significantly increased in SRV9-infected mice at 3 and 5 dpi (*, $P < 0.05$), whereas BD06 caused a breakdown of the BBB in the late stage of infection (Fig. 6).

Discussion

Rabies is a highly lethal but preventable disease caused by neurotropic RABV [20, 21]. RABV infects the CNS, causing fatal encephalitis and death [22]. However, the mechanism of rabies pathogenesis is still not completely understood, despite remarkable advances in the past several years. Animals infected with wt RABV do not develop VNAs, whereas attenuated RABV strains induce high levels of VNAs [23]. In the present study, we compared the immune responses in mice after infection with the attenuated, non-pathogenic SRV9 strain or the highly pathogenic wt BD06 strain, which was isolated from a rabid dog. Consistent with a previous report [24], our study showed that IM injection of mice with SRV9 induced serum VNAs at 5 dpi. However, little to no VNA production was observed in the serum of wt RABV-infected mice until the ED, which is consistent with previous reports of infections in other animal species, such as dogs [11] and skunks [25].

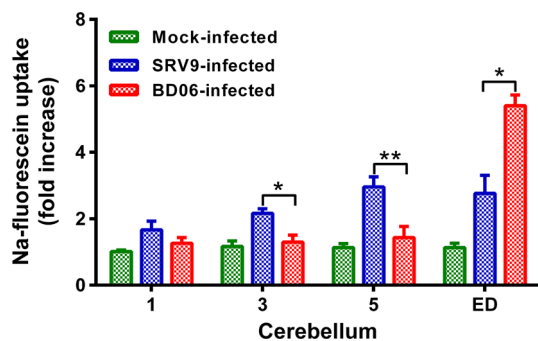


Fig. 6 A single IC dose of laboratory-attenuated SRV9 enhanced the BBB, and wt BD06 caused a breakdown of the BBB in the late stage of infection. Brains were removed from Na-fluorescein-treated mice at 1, 3, and 5 dpi and at the ED. BBB permeability was assessed by measuring Na-fluorescein content according to a standard curve. Compared with mock-infected control mice ($n = 4$), RABV-infected mice ($n = 8$) showed a significant increase in the amount of Na-fluorescein (*, $P < 0.05$)

Interestingly, the dynamic changes in the viral load in the CNS are related to serum VNA levels. Minimal VNA production was observed at the early stage of infection, during which SRV9 and BD06 virus replication is controlled by innate immunity. At 5 dpi, the SRV9-infected mice displayed increased VNA production, which contributed to virus elimination; however, the BD06-infected mice did not produce VNAs and thus developed rabies disease.

To gain further insight into the mechanism of RABV clearance from the CNS, a previous study used knockout ($JHD^{-/-}$) mice to study the role of different antiviral immune effectors in the CNS of mice that had cleared the attenuated RABV. They found that $JHD^{-/-}$ mice lacked B cells but had functional CD4 and CD8 T cells; furthermore, these mice were unable to clear the virus from the CNS and exhibited neurological signs, despite surviving the attenuated infection [26, 27]. In our previous study, we showed that antibodies or anti-RABV immunoglobulins did not enhance innate immunity in wt-infected mice but delayed latency without decreasing mortality. When RABV enters the CNS, enhancing innate immunity or administering anti-RABV antibodies or immunoglobulins cannot decrease the mortality associated with the virus [28, 29]. In this study, we showed that the attenuated SRV9 virus induced innate immunity, thereby limiting viral replication and leading to partial elimination of the virus. Furthermore, VNAs induced by the attenuated SRV9 virus cooperated with inflammatory cytokines to fully clear the virus. No activation of innate immunity was observed with the wt BD06 virus; thus, there was a massive increase in cytokines at the terminal stage of infection, and the mice died.

The attenuated RABV, but not the wt BD06 virus, can stimulate a humoral immune response. DCs can capture and retain unprocessed antigens and then directly transfer these antigens to naïve B cells to initiate antigen-specific antibody responses. Dubois et al. reported that small numbers (250 to 1,000) of DCs can directly stimulate the proliferation of and antibody production by activated B cells [30]. Cao et al. reported that regulatory DCs are responsible for B cell differentiation [31]. In our study, SRV9 infection induced DC differentiation and maturity, which stimulated B cell maturation and VNA production.

Although the mechanism by which different RABVs trigger and evade immune responses are unknown, studies indicate that laboratory-attenuated RABVs can trigger an innate immune response in the host, whereas wt RABV evades the immune response [7]. The use of recombinant RABVs expressing cytokines or chemokines that promote the activation of immune cells, including DCs and B cells, is correlated with greater VNA production and better protection from rabies [32–34]. In addition, these recombinant RABVs recruit more activated B cells in lymph nodes and

CD8 T cells in the peripheral blood, which enables virus clearance in the early stage of infection [33, 35]. The wt RABV evades the host immune response and invades the CNS while maintaining neuronal integrity [29] and failing to cross the BBB during infection [36]. T cell activity inhibits RABV replication, and the production of RABV-specific antibodies by infiltrating B cells (as opposed to circulating antibodies that leak across the BBB) is critical for virus elimination. These findings suggest that a pathogenic RABV infection may be treatable after the virus has reached the CNS, provided that the appropriate immune effectors can be targeted. In a previous study, mice lacking T and B cells could not clear RABV and died from the infection [26].

The innate immune response is the first line of defense against infectious agents. RABV harbors a mechanism for evading the host innate immune response [37]; for example, the multifunctional P genes antagonize IFN- β induction [10, 38]. Our results indicated that the P proteins from both SRV9 and wt BD06 had antagonistic activity against IFN; however, the inhibition was stronger with SRV9 than BD06, although the mechanism leading to this difference is unclear. RABV wt strains significantly inhibit I-kappa-B kinase ϵ (IKK ϵ)-inducible IRF-3-dependent IFN- β promoter activity to antagonize IFN signaling [39].

In summary, we demonstrated that either IC or IM infection of mice with the SRV9 strain of RABV led to viral replication in the CNS that induced both innate and adaptive immunity, both of which were beneficial for eliminating the virus. However, the wt BD06 virus failed to induce innate immunity, leading to death from rabies infection. A comparative analysis showed that the SRV9 virus more strongly antagonized IFN activity than the BD06 virus, indicating that there is no positive relationship between viral IFN antagonist activity and pathogenicity.

Acknowledgments This project was funded by the National Natural Science Foundation of China (31472176) and the Key Project of National Natural Science Foundation of China (30630049).

Compliance with ethical standards

Conflict of interest The authors declare that they have no competing interests.

References

- Shwiff S, Hampson K, Anderson A (2013) Potential economic benefits of eliminating canine rabies. *Antiviral Res* 98(2):352–356
- Feder HM Jr, Petersen BW, Robertson KL, Rupprecht CE (2012) Rabies: still a uniformly fatal disease? Historical occurrence, epidemiological trends, and paradigm shifts. *Curr Infect Dis Rep* 14:408–422
- Hooper DC, Morimoto K, Bette M, Weihe E, Koprowski H, Dietzschold B (1998) Collaboration of antibody and inflammation in clearance of rabies virus from the central nervous system. *J Virol* 72:3711–3719
- Appolinario CM, Jackson AC (2015) Antiviral therapy for human rabies. *Antivir Ther* 20:1–10
- Rubin J, David D, Willoughby RE Jr, Rupprecht CE, Garcia C, Guarda DC, Zohar Z, Stamler A (2009) Applying the Milwaukee protocol to treat canine rabies in Equatorial Guinea. *Scand J Infect Dis* 41:372–375
- Takeuchi O, Akira S (2009) Innate immunity to virus infection. *Immunol Rev* 227:75–86
- Wang ZW, Sarmiento L, Wang Y, Li XQ, Dhingra V, Tseggai T, Jiang B, Fu ZF (2005) Attenuated rabies virus activates, while pathogenic rabies virus evades, the host innate immune responses in the central nervous system. *J Virol* 79:12554–12565
- Gnanadurai CW, Yang Y, Huang Y, Li Z, Leyson CM, Cooper TL, Platt SR, Harvey SB, Hooper DC, Faber M, Fu ZF (2015) Differential host immune responses after infection with wild-type or lab-attenuated rabies viruses in dogs. *PLoS Negl Trop Dis* 9:e0004023
- Pestka S, Krause CD, Walter MR (2004) Interferons, interferon-like cytokines, and their receptors. *Immunol Rev* 202:8–32
- Brzozka K, Finke S, Conzelmann KK (2005) Identification of the rabies virus alpha/beta interferon antagonist: phosphoprotein P interferes with phosphorylation of interferon regulatory factor 3. *J Virol* 79:7673–7681
- Brzozka K, Finke S, Conzelmann KK (2006) Inhibition of interferon signaling by rabies virus phosphoprotein P: activation-dependent binding of STAT1 and STAT2. *J Virol* 80:2675–2683
- Ministry of Science and Technology of the People's Republic of China. http://www.most.gov.cn/fggw/zfwj/zfwj2006/zf06wj/zf06bfw/200609/t20060930_54196.htm. Accessed 30 Sept 2006
- Zhao J, Wang S, Zhang S, Liu Y, Zhang J, Zhang F, Mi L, Hu R (2014) Molecular characterization of a rabies virus isolate from a rabid dog in Hanzhong District, Shaanxi Province, China. *Arch Virol* 159:1481–1486
- Zhao J, Liu Y, Zhang S, Fang L, Zhang F, Hu R (2014) Experimental oral immunization of ferret badgers (*Melogale moschata*) with a recombinant canine adenovirus vaccine CAV-2-E3Delta-RGP and an attenuated rabies virus SRV9. *J Wildl Dis* 50:374–377
- Meslin FX, Kaplan MM, Koprowski H (1996) Laboratory techniques in rabies, 4th edn. World Health Organization, Geneva, pp 80–168
- Wong ML, Medrano JF (2005) Real-time PCR for mRNA quantitation. *Biotechniques* 39:75–85
- Deng HK, Unutmaz D, KewalRamani VN, Littman DR (1997) Expression cloning of new receptors used by simian and human immunodeficiency viruses. *Nature* 388:296–300
- Phares TW, Kean RB, Mikheeva T, Hooper DC (2006) Regional differences in blood–brain barrier permeability changes and inflammation in the apathogenic clearance of virus from the central nervous system. *J Immunol* 176:7666–7675
- Ito N, Moseley GW, Blondel D, Shimizu K, Rowe CL, Ito Y, Masatani T, Nakagawa K, Jans DA, Sugiyama M (2010) Role of interferon antagonist activity of rabies virus phosphoprotein in viral pathogenicity. *J Virol* 84:6699–6710
- Dietzschold B, Schnell M, Koprowski H (2005) Pathogenesis of rabies. *Curr Top Microbiol Immunol* 292:45–56
- Hemachudha T, Ugolini G, Wacharapluesadee S, Sungkarat W, Shuangshoti S, Laothamatas J (2013) Human rabies: neuropathogenesis, diagnosis, and management. *Lancet Neurol* 12:498–513

22. World Health Organization (2013) WHO expert consultation on rabies. Second report. Technical report series, back cover, pp 1–139
23. Gnanadurai CW, Zhou M, He W, Leyson CM, Huang CT, Salyards G, Harvey SB, Chen Z, He B, Yang Y, Hooper DC, Dietzschold B, Fu ZF (2013) Presence of virus neutralizing antibodies in cerebral spinal fluid correlates with non-lethal rabies in dogs. *PLoS Negl Trop Dis* 7:e2375
24. Schutsky K, Curtis D, Bongiorno EK, Barkhouse DA, Kean RB, Dietzschold B, Hooper DC, Faber M (2013) Intramuscular inoculation of mice with the live-attenuated recombinant rabies virus TriGAS results in a transient infection of the draining lymph nodes and a robust, long-lasting protective immune response against rabies. *J Virol* 87:1834–1841
25. Tolson ND, Charlton KM, Lawson KF, Campbell JB, Stewart RB (1988) Studies of ERA/BHK-21 rabies vaccine in skunks and mice. *Can J Vet Res = Revue canadienne de recherche veterinaire* 52:58–62
26. Hooper DC, Phares TW, Fabis MJ, Roy A (2009) The production of antibody by invading B cells is required for the clearance of rabies virus from the central nervous system. *PLoS Negl Trop Dis* 3:e535
27. Hooper DC, Roy A, Barkhouse DA, Li J, Kean RB (2011) Rabies virus clearance from the central nervous system. *Adv Virus Res* 79:55–71
28. Liao PH, Yang HH, Chou PT, Wang MH, Chu PC, Liu HL, Chen LK (2012) Sufficient virus-neutralizing antibody in the central nerve system improves the survival of rabid rats. *J Biomed Sci* 19:61
29. Roy A, Hooper DC (2008) Immune evasion by rabies viruses through the maintenance of blood–brain barrier integrity. *J Neurovirol* 14:401–411
30. Dubois B, Bridon JM, Fayette J, Barthelemy C, Banchereau J, Caux C, Briere F (1999) Dendritic cells directly modulate B cell growth and differentiation. *J Leukoc Biol* 66:224–230
31. Qian L, Qian C, Chen Y, Bai Y, Bao Y, Lu L, Cao X (2012) Regulatory dendritic cells program B cells to differentiate into CD19hiFcgammaIIbhi regulatory B cells through IFN-beta and CD40L. *Blood* 120:581–591
32. Barkhouse DA, Garcia SA, Bongiorno EK, Lebrun A, Faber M, Hooper DC (2015) Expression of interferon gamma by a recombinant rabies virus strongly attenuates the pathogenicity of the virus via induction of type I interferon. *J Virol* 89:312–322
33. Wen Y, Wang H, Wu H, Yang F, Tripp RA, Hogan RJ, Fu ZF (2011) Rabies virus expressing dendritic cell-activating molecules enhances the innate and adaptive immune response to vaccination. *J Virol* 85:1634–1644
34. Zhou M, Wang L, Zhou S, Wang Z, Ruan J, Tang L, Jia Z, Cui M, Zhao L, Fu ZF (2015) Recombinant rabies virus expressing dog GM-CSF is an efficacious oral rabies vaccine for dogs. *Oncotarget* 6:38504–38516
35. Wang Y, Tian Q, Xu X, Yang X, Luo J, Mo W, Peng J, Niu X, Luo Y, Guo X (2014) Recombinant rabies virus expressing IFNalpha1 enhanced immune responses resulting in its attenuation and stronger immunogenicity. *Virology* 468–470:621–630
36. Roy A, Phares TW, Koprowski H, Hooper DC (2007) Failure to open the blood–brain barrier and deliver immune effectors to central nervous system tissues leads to the lethal outcome of silver-haired bat rabies virus infection. *J Virol* 81:1110–1118
37. Lafon M (2011) Evasive strategies in rabies virus infection. *Adv Virus Res* 79:33–53
38. Rieder M, Brzozka K, Pfaller CK, Cox JH, Stitz L, Conzelmann KK (2011) Genetic dissection of interferon-antagonistic functions of rabies virus phosphoprotein: inhibition of interferon regulatory factor 3 activation is important for pathogenicity. *J Virol* 85:842–852
39. Masatani T, Ozawa M, Yamada K, Ito N, Horie M, Matsuu A, Okuya K, Tsukiyama-Kohara K, Sugiyama M, Nishizono A (2015) Contribution of the interaction between rabies virus P protein and IKKepsilon to the inhibition of type I interferon induction signaling. *J Gen Virol* 97:316–326